Journal of the Serbian Chemical Society
JSCS-info@shd.org.rs • www.shd.org.rs/JSCS
J. Serb. Chem. Soc. *81* (3) 291–306 (2016)
JSCS–4847
UDC 546.815'47'56:681.5.017+621.385.833:544.654.2:66.012
Original Scientific paper

The shape of the polarization curve and diagnostic criteria for control of the metal electrodeposition process

KONSTANTIN I. POPOV[1,2], PREDRAG M. ŽIVKOVIĆ[1], BOJAN JOKIĆ[1] and NEBOJŠA D. NIKOLIĆ[2#*]

[1]*Faculty of Technology and Metallurgy, University of Belgrade, Karnegijeva 4, P. O. Box 3503, 11001 Belgrade and* [2]*Institute of Chemistry, Technology and Metallurgy, Department of Electrochemistry, University of Belgrade, Njegoševa 12, P. O. Box 473, 11001 Belgrade, Serbia*

(Received 17 July, revised and accepted 17 September 2015)

Abstract: The simulated shapes of the polarization curves were correlated with the type of metal electrodeposition process control as a function of the ratio of the exchange current density to the limiting diffusion current density (j_0/j_L). Diagnostic criteria based on the j_0/j_L ratios were established. For $j_0/j_L > 100$, the system is under the ohmic control. In the range $1 < j_0/j_L \leq 100$, there is mixed ohmic–diffusion control. Pure diffusion control appears in the range $0.1 < j_0/j_L \leq 1$. For $j_0/j_L \leq 0.1$, the system is activation controlled at low overpotentials. The proposed diagnostic criteria were verified by comparison of the simulated curves with experimentally recorded ones and by morphological analysis of deposits obtained under the different types of control of the metal electrodeposition process.

Keywords: lead; zinc; copper; simulation; morphology; scanning electron microscopy.

INTRODUCTION

Morphology, as the most important characteristic of electrodeposited metals, mainly depends on the kinetic parameters during the electrodeposition process and on the overpotential or current density applied.[1] Furthermore, the composition of the electroplating solution, temperature of electrolysis and the type of working electrode strongly affect the final morphology of an electrodeposited metal. The morphology of an electrodeposited metal depends also on the deposition time until the deposit has attained its final form.

* Corresponding author. E-mail:nikolic@ihtm.bg.ac.rs
# Serbian Chemical Society member.
doi: 10.2298/JSC150717076P

According to their general kinetic behavior in aqueous solution, metals can be classified into three classes.[2,3] These classes are:

a) Class I, so-called normal metals: Pb, Sn, Tl, Cd, Hg, Ag (simple electrolytes) and Zn. These metals have characteristic low melting points and high exchange current densities (j_0 > 1 A dm^{-2}; j_0 is the exchange current density). In addition, they show high overpotentials for hydrogen discharge.

b) Class II, intermediate metals: Cu, Au and Ag (complex electrolytes). These metals are characterized by moderate melting points, medium exchange current densities (j_0 in the interval from 10^{-2} to 1 A dm^{-2}) and lower hydrogen discharge overpotentials.

c) Class III, inert metals: Fe, Co, Ni, Mn, Cr and Pt. These metals have high melting points, low exchange current densities and very low hydrogen discharge overpotentials. For this class of metals, j_0 is between 10^{-2} and 10^{-12} A dm^{-2}.

The formation of individual and regular grains at lower and dendrites at higher overpotentials is characteristic of electrodeposition processes having extremely large exchange current densities.[1] Spongy deposits are formed at lower overpotentials and dendrites at higher ones during the electrodeposition of metals characterized by large exchange current densities. Finally, compact deposits are obtained at lower overpotentials, while both dendritic and spongy–dendritic deposits are formed at higher overpotentials during the electrodeposition of metals characterized by medium and low exchange current densities.

Obviously, the morphology of metal electrodeposits is strictly correlated with the type of control of the electrodeposition process. For example, the activation-controlled electrodeposition of copper produces large grains with relatively well-defined crystal shapes. This occurs at overpotentials belonging to the region of Tafel linearity.[4,5] At overpotentials situated between the end of Tafel linearity and the beginning of the limiting diffusion current density plateau (the mixed activation–diffusion control), morphological forms are created by the mass transfer limitations and large grains are not formed.[6,7] Dendrites are formed at overpotentials within the plateau of the limiting diffusion current density, and at the higher ones when there is no hydrogen evolution or hydrogen evolution is not sufficient to affect the hydrodynamic conditions in the near-electrode layer.[8,9] The above consideration is valid for all electrodeposition processes characterized by medium and low values of the exchange current density, in the absence of a noticeable hydrogen evolution reaction.[9] In the presence of strong hydrogen evolution, honeycomb-like deposits are formed.[9]

On the other hand, electrodeposition of metals characterized by high values of the exchange current density occurs under conditions of ohmic, mixed ohmic–diffusion and only diffusion control of the electrodeposition.[10–12] The formation of spongy deposits at lower and dendrites at higher overpotentials was explained by the assumption of diffusion-controlled electrodeposition over the whole

range of overpotentials.[10] The linear dependence of the current density on the overpotential was ascribed to ohmic control,[11] and the regular grains were formed by electrodeposition under this control. In this way, the formation of regular particles at lower and dendritic deposits at higher overpotentials under mixed ohmic–diffusion control could be explained.[12]

Simultaneously, the shape of the polarization curves strongly depends on the values of the exchange current density. The limiting diffusion current density (j_L) values are another important characteristic of electrodeposition systems, indicating to a strong dependence of the shape of the polarization curves on the j_0/j_L ratios. Since the effect of a continuous change in the ratios of the exchange current density to the limiting diffusion current density (j_0/j_L) on the shape of the polarization curves can only be obtained by digital simulation, the software MathLab will be used in this study to examine the dependence of the shape of polarization curve on the j_0/j_L ratio. This will enable the establishment of diagnostic criteria relating the shape of the polarization curves through j_0/j_L ratios with the type of electrodeposition control. The proposed diagnostic criteria will be verified by comparison with experimentally recorded polarization curves and by the morphologies of deposits obtained under different types of electrodeposition control.

EXPERIMENTAL

Polarization curves for electrodeposition of lead, zinc and copper were recorded from the following solutions: a) 0.050 M $Pb(NO_3)_2$ in 2.0 M $NaNO_3$, b) 0.10 M $Pb(NO_3)_2$ in 2.0 M $NaNO_3$, c) 0.20 M $Pb(NO_3)_2$ in 2.0 M $NaNO_3$, d) 0.40 M $Pb(NO_3)_2$ in 2.0 M $NaNO_3$, e) 0.45 M $Pb(NO_3)_2$ in 2.0 M $NaNO_3$, f) 0.10 M $ZnSO_4$ in 2.0 M NaOH and g) 0.10 M $CuSO_4$ in 0.50 M H_2SO_4.

The experimental procedure for recording the Pb polarization curves is given in the literature.[13,14]

For the morphological analysis of deposits, lead, copper and zinc were electrodeposited potentiostatically at overpotentials of 10, 50 and 100 mV (Pb), 90, 210, 650 and 1000 mV (Cu) and 45 and 100 mV (Zn). The times of electrodeposition are indicated in the Figure captions.

Double-distilled water and analytical grade chemicals were used for the preparation of solutions used for the electrodeposition of all metals. All experiments were performed in an open cell at room temperature on vertical cylindrical copper electrodes. The geometric surface area of copper electrodes was 0.25 cm^2. The reference and counter electrodes were of the same metals as the deposited one. The counter-electrodes were metallic foils with 0.80 dm^2 surface area placed close to the cell walls. The reference electrodes, the tips of which were positioned at a distance of about 0.2 cm from the surface of the working electrodes, were wires of the corresponding metals. The working electrodes were placed in the centre of a cell, at the same location for each experiment.

Morphologies of lead, copper and zinc deposits were examined using a scanning electron microscope Tescan Digital Microscopy.

Digital simulation was realized using MathLab software.

RESULTS AND DISCUSSION

The equation of the polarization curve taking the concentration dependence of j_0 into account and the linear dependence of j_0 on the c_s/c_0 ratio is given by Eq. (1):[11,15,16]

$$j = \frac{j_0 (f_c - f_a)}{1 + \frac{j_0}{j_L}(f_c - f_a)} \tag{1}$$

To enable a digital simulation of the equation of the polarization curve for different j_0/j_L ratios, Eq. (1) can be re-written in the form:

$$\frac{j}{j_L} = \frac{\frac{j_0}{j_L}(f_c - f_a)}{1 + \frac{j_0}{j_L}(f_c - f_a)} \tag{2}$$

being valid for all j_0/j_L ratios and overpotentials. For this reason, this form will be used in the discussion of the effect of the j_0/j_L ratio on the shape of the polarization curves. Using the current density–overpotential relationship and the procedure for the determination of the ohmic potential drop, the polarization curves for electrodeposition processes can be successfully simulated.[11,17]

In Eqs. (1) and (2), j is the current density, and:

$$f_c = 10^{\frac{\eta}{b_c}} \text{ and } f_a = 10^{-\frac{\eta}{b_a}} \tag{3}$$

where b_c and b_a are the cathodic and anodic Tafel slopes and η is the overpotential.

Equations (1) and (2) are modified for use in the electrodeposition of metals using the values of the cathodic current density and overpotential as positive. In Eqs. (1) and (2), the ohmic potential drop is not included in the overpotential values. Equations (1) and (2) are operative if the IR error is eliminated by using electronic devices that distinguish the superfast change in potential that occurs in this IR portion, when the current density is switched on and off from the slower change of the electrode potential itself, when the charging of the interfacial capacitor takes time.[17] In this way, polarization curves that do not include the ohmic potential drop can be simulated using Eq. (2).

In any other case, the measured value of overpotential, η_m, includes the ohmic potential drop, which is given by:

$$\eta_m = \eta + j\frac{L}{\kappa} \tag{4}$$

where L is the length of the electrolyte column between the tip of a liquid capillary and the electrode and κ is the specific conductivity of the electrolyte. Hence, the polarization curves that include the ohmic potential drop can be simulated by using Eqs. (2) and (4).

Simulation of polarization curves

The polarization curves without inclusion of the ohmic potential drop for different values of the j_0/j_L ratio for both one and two electron reactions are shown in Fig. 1. They were obtained using Eq. (2) for different j_0/j_L ratios and

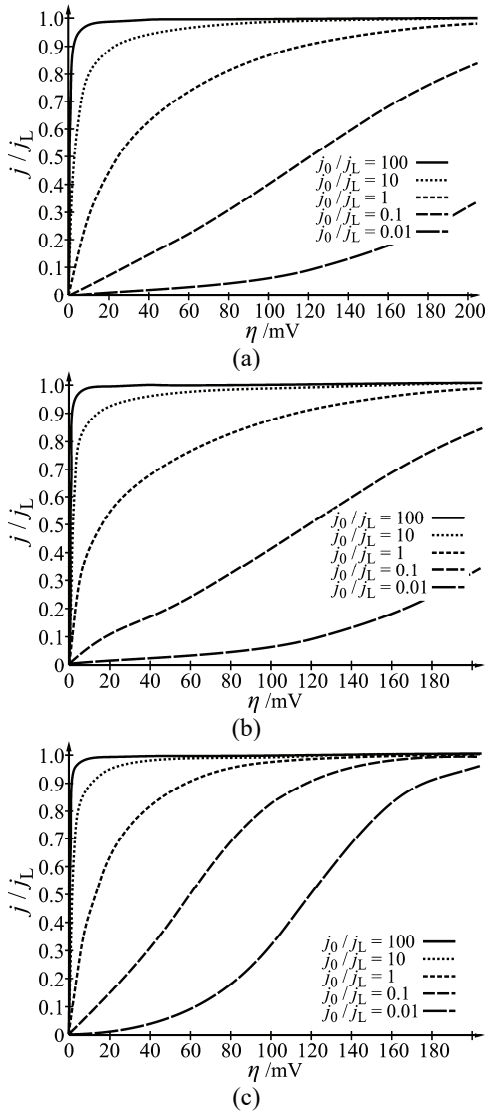

Fig. 1. Dependencies j/j_L–η calculated using Eqs. (2) and (3) for different values of the j_0/j_L ratio: a) b_a = 120 mV dec^{-1}, b_c = = 120 mV dec^{-1}, b) b_a = 40 mV dec^{-1}, b_c = = 120 mV dec^{-1} and c) b_a = 60 mV dec^{-1}, b_c = 60 mV dec^{-1}.

for different η, b_a and b_c values in dependence of the mechanism of the electrodeposition reactions. From Fig. 1, it is clear that these dependencies are similar to each other for large values of the j_0/j_L ratio and at any low value of overpotential. For this reason, the polarization curves without the ohmic potential drop included are not suitable and, hence, will not be treated further.

The simulated polarization curves with the ohmic potential drop included are shown in Fig. 2. They were obtained using the same data as those shown in

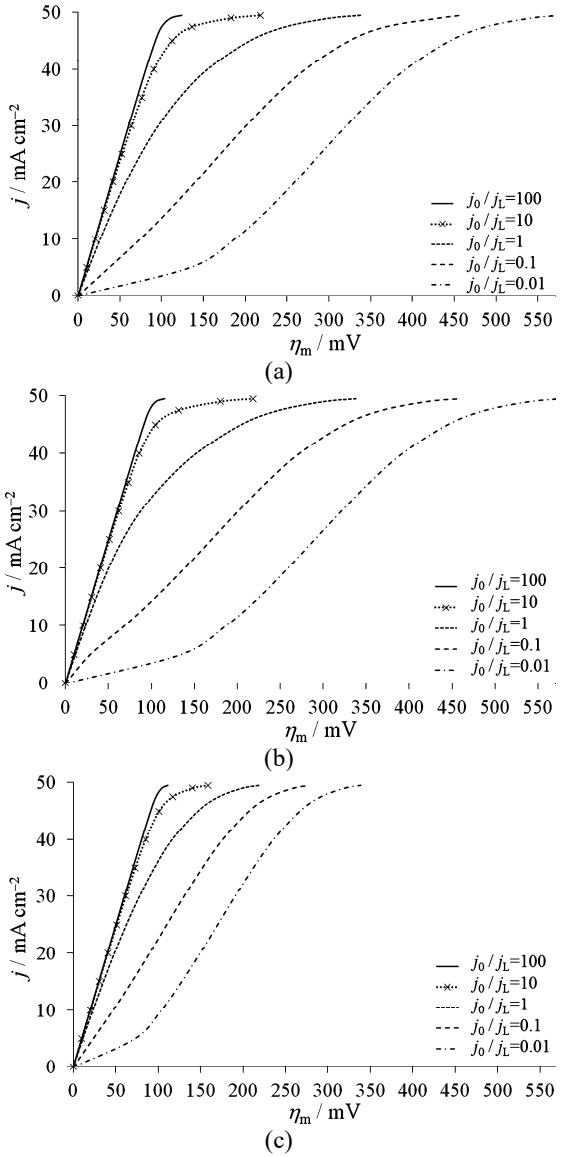

Fig. 2. Dependencies j–η_m calculated using Eqs. (2)–(4) and different values of the j_0/j_L ratio for j_L = 50 mA cm^{-2}, L = 0.2 cm and κ = 0.1 S cm^{-2}; a), b) and c) as in the captions in Fig. 1.

Fig. 1 and for j_L = 50 mA cm^{-2}, L = 0.2 cm and κ = 0.1 S cm^{-1}. In all cases for j_0/j_L = 100, there is a linear dependence of the current density on overpotential up to j = 45 mA cm^{-2}, or to $j/j_L \approx 0.9$. In these cases, the overpotential without the ohmic potential drop included (see Fig. 1) is very low and the measured overpotential is practically equal to the ohmic potential drop between the working and the reference electrodes. Hence, for $j_0/j_L > 100$ there is ohmic control of the electrodeposition process. It is obvious that the shape of the linear part of polarization curve does not depend on the mechanism of the electrode reaction.

The polarization curves consist of two parts in the mixed ohmic–diffusion controlled electrodeposition.[12] The first part corresponds to ohmic control (it is the linear part), and the second one corresponds to diffusion control (Fig. 3a–c). The length of the ohmic part on the polarization curve decreases with decreasing values of the j_0/j_L ratio. The simulated polarization curves shown in Fig. 3a–c were obtained under the same conditions as those shown in Fig. 2, but for j_0/j_L ratios between 10 and 100. Assuming that the diffusion control of the electrodeposition process becomes visible at η_m = 0.5 mV from the linear dependence of the current density on the overpotential (see Fig. 3d), the values of the current density $j_{0.5}$ were determined from Fig. 3, and the dependencies of $j_{0.5}/j_L$ on the j_0/j_L ratio are shown in Fig. 4 and given in Table I. Hence, the current density $j_{0.5}$ corresponds to the values of current density at 0.5 mV from the linear part on polarization curve. It could be seen from Fig. 4 and Table I that the linear part of the polarization curve vanishes at j_0/j_L = 1. Hence, there is mixed ohmic–diffusion control in the interval $1 < j_0/j_L \leq 100$.

At values of the ratio j_0/j_L lower than 1, complete diffusion control of the electrodeposition process arises at all overpotentials. The lower limit of the region of complete diffusion control can be determined as follows: it is obvious that the convex shape of the polarization curve characterizes diffusion control of the deposition process and the concave one the activation control of the deposition process. The j/j_L ratio as function of η is shown in Fig. 1 and j as a function of η_m in Fig. 2. In both cases, the convex shape of the curves changes into a concave one at $j_0/j_L \approx 0.1$, meaning that the diffusion control changes into an activation one at the beginning of the polarization curve at low η and η_m. At larger overpotentials, diffusion control occurs. Hence, diffusion control at all overpotentials appears at $0.1 < j_0/j_L \leq 1$, while activation control appears at $j_0/j_L \leq 0.1$ at low overpotentials.

It can be seen from Figs. 1 and 2 that the same conclusion could be derived for the polarization curves with and without inclusion of the ohmic overpotential drop. The simulated polarization curves with included ohmic drop were calculated using data for a 1 M solution of a typically fully dissociated electrolyte without supporting electrolyte.[17] It is obvious that for less concentrated solutions with a supporting electrolyte (mainly some acid or base), the ohmic potential drop

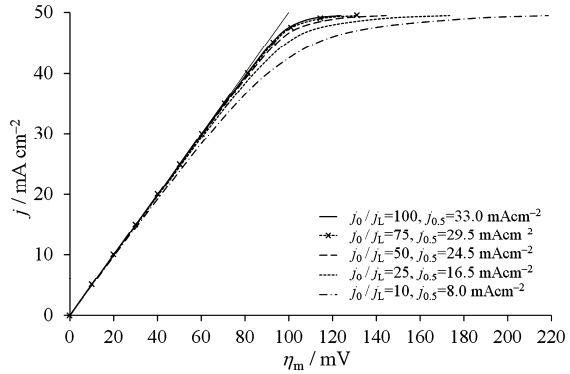

(a)

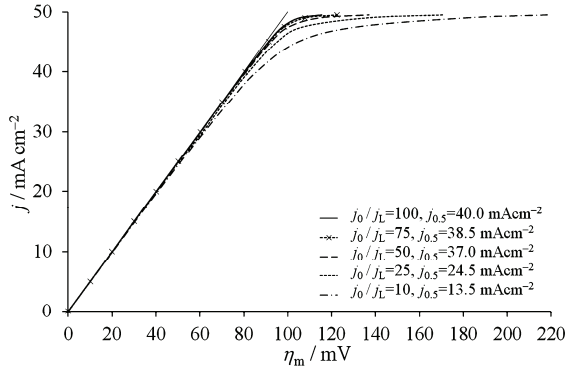

(b)

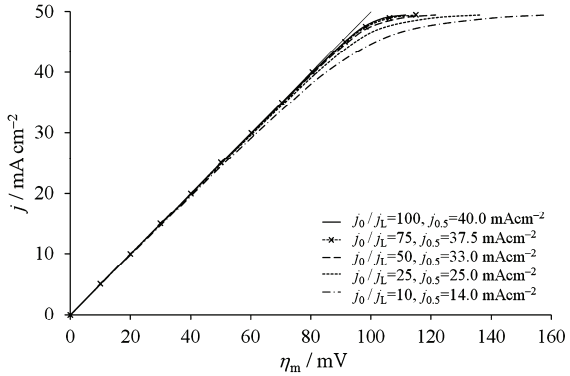

(c)

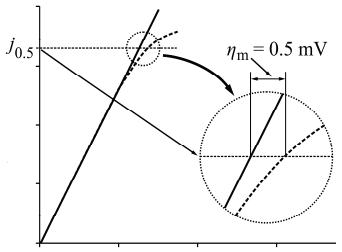

(d)

Fig. 3. Dependencies j–η_m for $10 \leq \leq j_0/j_L \leq 100$ calculated as those in Fig. 2; a), b) and c) as in the captions in Fig. 1; d) the manner for the determination of $j_{0.5}$.

can be neglected. For this reason, η will be used instead of η_m, except for some indicated special cases.

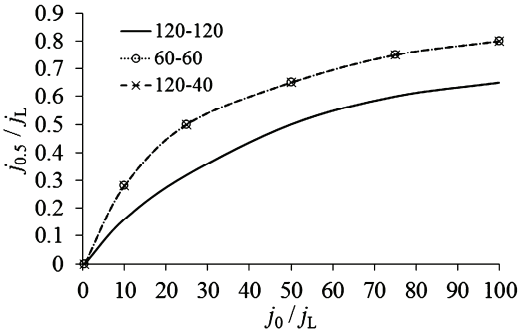

Fig. 4. Dependencies of the $j_{0.5}/j_L$ ratio on the j_0/j_L ratio; a), b) and c) as in the captions in Fig. 1.

TABLE I. Calculated value of $j_{0.5}$, mA cm^{-2}, as a function of the j_0/j_L ratio; a), b) and c) as in the caption of Fig. 1

j_0/j_L	Notation from Fig. 1		
	a	b	c
10	8.0	13.5	14.0
25	16.5	24.5	25.0
50	24.5	37.0	33.0
75	29.5	38.5	37.5
100	33.0	40.0	40.0

Experimental verification of the simulated polarization curves with the ohmic potential drop included

The nearest experimental curves to the simulated curves for j_0/j_L =100 (full ohmic control) and $1 < j_0/j_L \leq 100$ (mixed ohmic–diffusion control) were recorded during lead electrodeposition processes because the electrodeposition of lead occurs under conditions of mixed ohmic–diffusion control or even full ohmic control.[12] Lead is characterized by an extremely high value of the exchange current density ($j_0 \rightarrow \infty$; fast electrochemical processes), and there is no precise and unique way for the determination of the values of the exchange current density. For this reason, comparison of simulated and experimentally recorded polarization curves could be an excellent auxiliary method for an approximate estimation of the exchange current density of lead, as well as the other metals from the group of normal metals. The ratio of ohmic to the overall control of the electrodeposition increases with increasing concentration of Pb^{2+} so that the electrodeposition process becomes fully ohmic controlled at high concentrations of Pb^{2+}.[12]

Typical Pb polarization curves recorded from solutions of different Pb^{2+} concentrations are shown in Fig. 5. The end of the ohmic control is denoted by a solid vertical line, while the inflection point is denoted by dotted vertical line. The linear dependence of the current density on the overpotential up to the inflection point corresponds to full ohmic control, and the current density at the

inflection point corresponds to the limiting diffusion current density.[12] As seen from Fig. 5a, the condition for full ohmic control is fulfilled with a concentration of Pb^{2+} ions of 0.45 M (the linear dependence of j–η up to the inflection point) and furthermore with 0.40 M because the linear dependence of j–η is up to about $j/j_L \approx 0.9$.

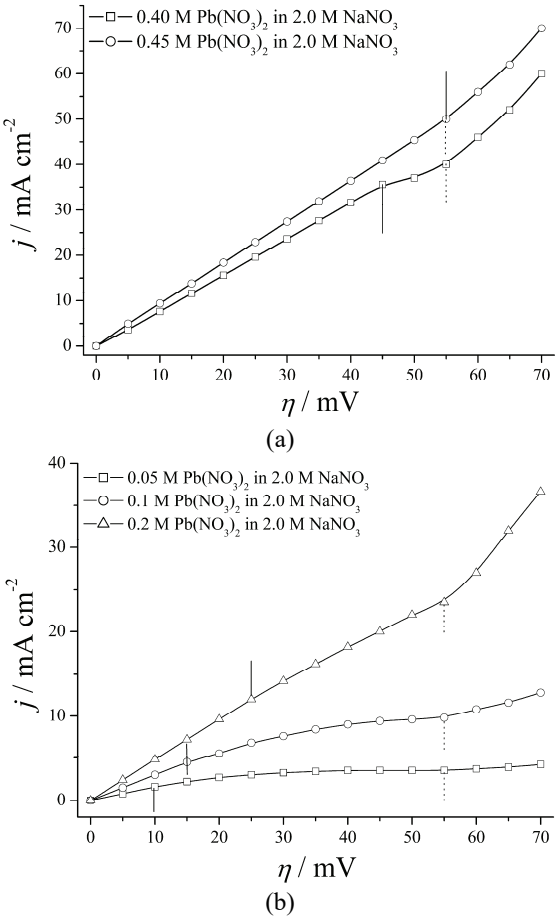

Fig. 5. The polarization curves for lead electrodeposition from: a) 0.40 and 0.45 M and b) 0.050, 0.10 and 0.20 M $Pb(NO_3)_2$ in 2.0 M $NaNO_3$.

With decreasing concentration of Pb^{2+} (Fig. 5b), the electrodeposition of Pb occurs under conditions of mixed ohmic–diffusion control. After the inflection point, the electrodeposition system remains under diffusion control and the rapid increase in current density with further increasing of overpotential is due to a strong increase in the surface area of the electrode caused by instantaneous formation and growth of dendrites. The ratios of j/j_L, where j corresponds to the end of the linear dependence and j_L to the inflection point on the polarization curve

were approximately 0.51, 0.46 and 0.46 for 0.20, 0.10 and 0.050 M Pb^{2+}, respectively.

Typical surface morphologies of lead obtained from 0.10 M $Pb(NO_3)_2$ in 2.0 M $NaNO_3$ are shown in Fig. 6. Regular hexagonal particles were formed by electrodeposition under ohmic control (Fig. 6a; η = 10 mV). The elongated irregular particles (precursors of dendrites) and dendrites of the different shape (needle-like and „tooth of saw"-like dendrites) were formed under diffusion control before (Fig. 6b; η = 50 mV) and after (Fig. 6c; η = 100 mV) the inflection point on the polarization curve. Following the classical Wranglen definition of a dendrite,[18,19] the dendrites of Pb belong to 2D (two-dimensional) primary (P) type dendrites. The lead dendrites were very similar to those obtained in silver electrodeposition processes from nitrate electrolytes,[20-22] indicating the strong dependence of the shape of dendrites on the affiliation to the determined group of metals.

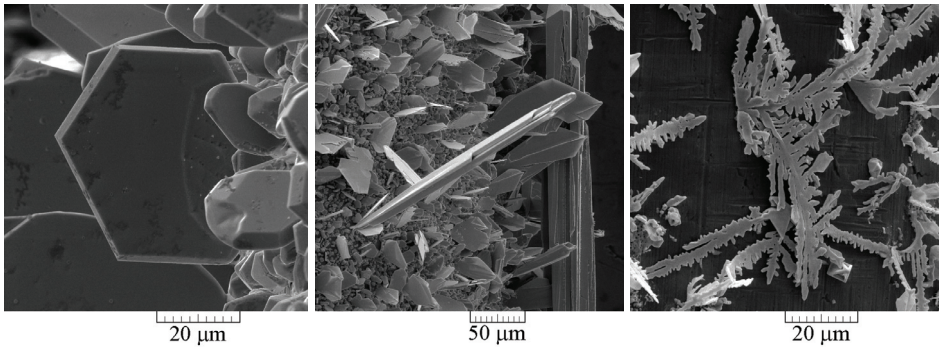

Fig. 6. The typical surface morphologies of lead electrodeposited from 0.10 M $Pb(NO_3)_2$ in 2.0 M $NaNO_3$ at overpotentials of: a) η = 10 mV (ohmic control); time of the electrodeposition (t), t = 25 min, b) η = 50 mV (diffusion control before the inflection point), t = 210 s, and c) η = 100 mV (diffusion control after the inflection point), t = 140 s.

Zinc also belongs to the group of normal metals characterized by $j_0 \rightarrow \infty$, but the shape of the polarization curve was completely different from those characteristic for Pb. A typical Zn polarization curve obtained from 0.10 M $ZnSO_4$ in 2.0 M NaOH is shown in Fig. 7a, from which it could be seen that is no the ohmic controlled part on this polarization curve. After the initial part determined by a low nucleation rate, the shape of polarization curve takes a convex shape up to attainment of the plateau of the limiting diffusion current density. Comparing this shape of the polarization curve with those of the simulated ones, it is clear that Zn is a „slower metal" than Pb, with the ratio $j_0/j_L < 1$.

The morphology of the electrodeposited Zn was also completely different from the one observed during electrodeposition of Pb. Instead of the regular

grains formed during Pb electrodeposition, spongy particles were formed at overpotentials belonging to the convex shape on the polarization curve (Fig. 7b; η = 45 mV). Simultaneously, dendrites were electrodeposited on the plateau of the limiting diffusion current density (Fig. 7c; η = 100 mV).

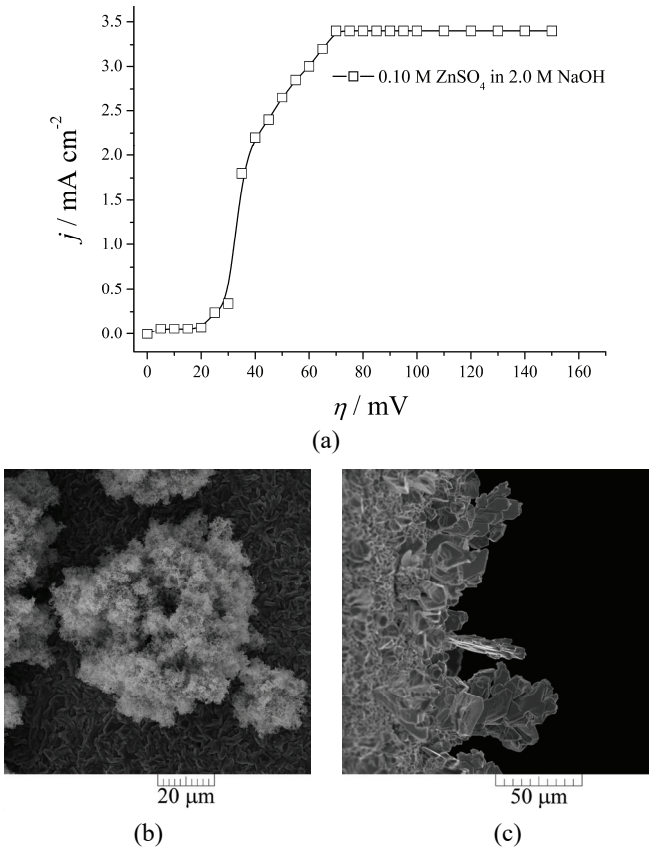

Fig. 7. a) The polarization curve for Zn electrodeposition from 0.10 M $ZnSO_4$ in 2.0 M NaOH, and the typical surface morphologies obtained at overpotentials of: b) η = 45 mV (zone of the rapid increase in the current density with increasing overpotential), t = 60 min, and c) η = 100 mV (plateau of the limiting diffusion current density), t = 50 min.

A further lowering the exchange current density led to a further change in the shape of the polarization curve. As result of this, the initial part of the polarization curve transformed from a convex (diffusion control) to a concave (activation control) one at approximately $j_0/j_L \leq 0.1$. A typical representative of this group of metals is copper. Namely, Cu belongs to the group of the intermediate metals characterized by medium values of the exchange current density.[2,3] The polarization curve obtained from a solution containing 0.10 M $CuSO_4$ in 0.50 M

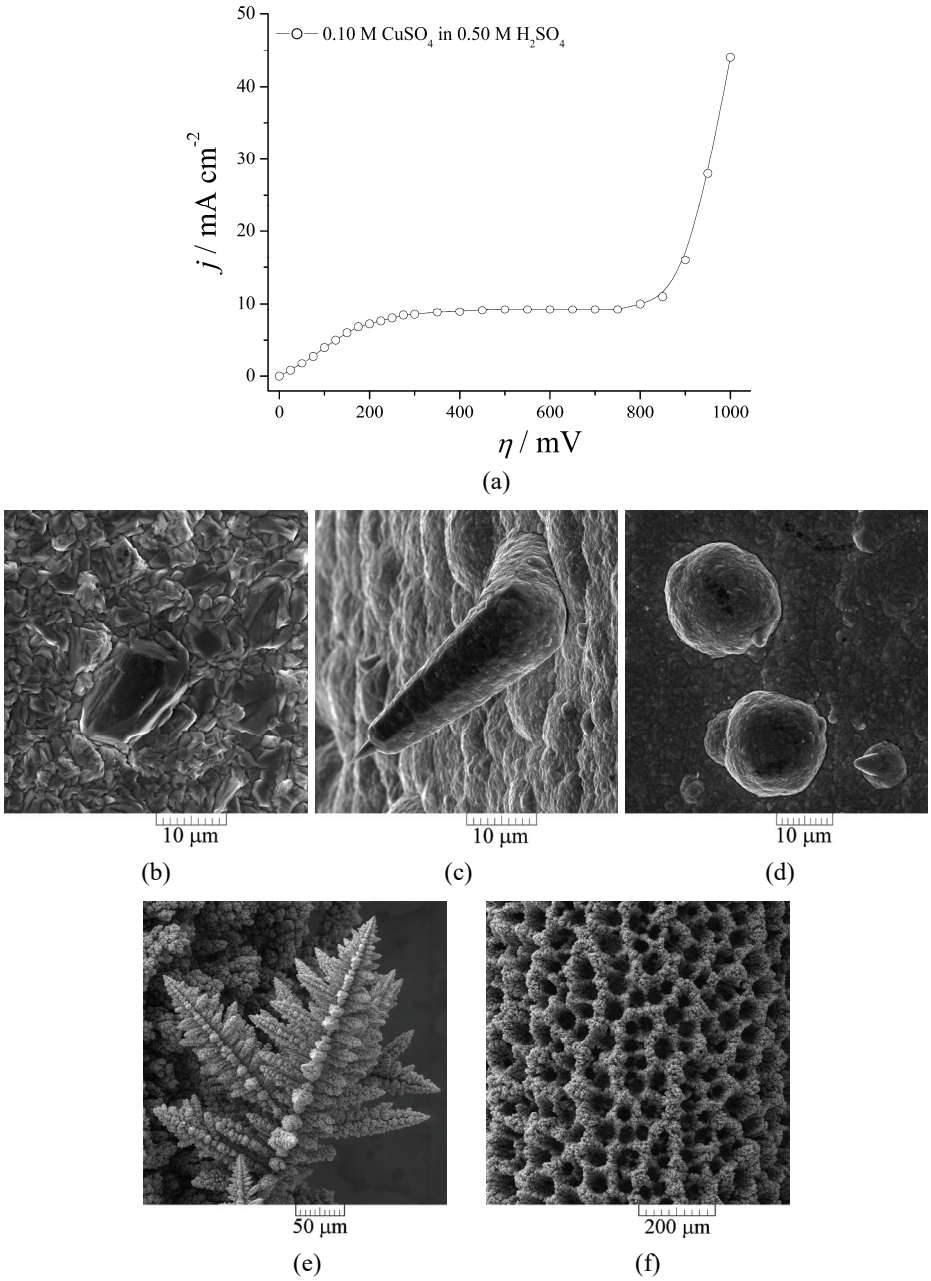

Fig. 8. a) The polarization curve for Cu electrodeposition from 0.10 M $CuSO_4$ in 0.50 M H_2SO_4, and the typical surface morphologies obtained in the different types of control: b) activation, η = 90 mV; t = 120 min, c) and d) activation–diffusion, η = 210 mV; t = 45 min, e) diffusion, η = 650 mV; t = 52 min, and f) zone of the fast increase of current density with overpotential, η = 1000 mV; t = 120 s.

H_2SO_4 is shown in Fig. 8a. For this solution,[1] j_0 = 0.11 mA cm^{-2} and j_L = 9.2 mA cm^{-2} and hence j_0/j_L = 0.012. This polarization curve consists of four parts: a) activation, b) mixed activation–diffusion, c) diffusion, and d) the zone of the fast increase of current density with overpotential. Electrodeposition in each of these regions produces characteristic surface morphologies. Large grains are obtained in the activation-controlled electrodeposition (Fig. 8b). The carrot-like (Fig. 8c) and globular forms (Fig. 8d) are formed in the mixed activation–diffusion control. The 3D (three-dimensional) pine-like dendrites formed inside the plateau of the limiting diffusion current density are shown in Fig. 8e. The shape of the pine-like Cu dendrites was very similar to the Ag dendrites obtained from various types of complex electrolytes, such as those with the addition of ammonia,[22,23] tungstosilicate[24] and citric[25] acids, and to the Au dendrites.[26] In this way, a strong correlation between the surface morphologies and the affiliation to the determined group of metals was confirmed. Due to the lower overpotentials for the hydrogen evolution reaction, the effect of evolved hydrogen as a parallel reaction to copper electrodeposition at high overpotentials became visible in the zone of the fast increase in the current density with increasing overpotential. Honeycomb-like structures could be formed in this zone (Fig. 8f).

Finally, electrodeposition of metals from the group of inert metals occurs parallel with the hydrogen evolution reaction in the whole range of potentials and current densities. The corrected polarization curves could only be obtained after IR drop correction,[27] making their analysis out of scope of this investigation. Due to the vigorous hydrogen evolution, spongy-like and globular particles, as well as degenerate dendrites were formed.[28–30]

Nevertheless, correlation between the polarization characteristics and surface morphologies could be established. For example, the polarization curve for Cu (Fig. 8a) was very similar to the one for Ag obtained from an ammonium electrolyte.[23] This similarity of the polarization characteristics was accompanied by almost identical shapes of the dendrites obtained within the plateau of the limiting diffusion current density. On the other hand, the common characteristic of normal metals is the formation of dendrites starting from relatively small overpotentials. A lowering of the values of the exchange current density was accompanied by a shift of the beginning of diffusion control towards higher overpotentials of the electrodeposition and by a transition of the dendritic growth from 2D (two-dimensional) to 3D (three-dimensional).

CONCLUSIONS

The polarization curves for different ratios of the exchange current density to the limiting diffusion current density (j_0/j_L) were simulated. The correlation between the shape of polarization curve and the type of metal electrodeposition process control was established based on these ratios. Four diagnostic criteria

based on the j_0/j_L ratio were established: a) $j_0/j_L > 100$ – ohmic control, b) $1 < j_0/j_L \leq 100$ – mixed ohmic–diffusion control, c) $0.1 < j_0/j_L \leq 1$ – diffusion control and d) $j_0/j_L \leq 0.1$ – the activation control at low overpotentials. The verification of the proposed diagnostic criteria was successfully realized by comparison with experimentally obtained polarization curves and by surface analysis of the deposits obtained in the different types of control of the metal electrodeposition process.

Acknowledgement. The work was supported by the Ministry of Education, Science and Technological Development of the Republic of Serbia under the research project: "Electrochemical synthesis and characterization of nanostructured functional materials for application in new technologies" (No. 172046).

ИЗВОД

ОБЛИК ПОЛАРИЗАЦИОНЕ КРИВЕ И ДИЈАГНОСТИЧКИ КРИТЕРИЈУМИ ЗА КОНТРОЛУ ПРОЦЕСА ЕЛЕКТРОХЕМИЈСКОГ ТАЛОЖЕЊА МЕТАЛА

КОНСТАНТИН И. ПОПОВ[1,2], ПРЕДРАГ М. ЖИВКОВИЋ[1], БОЈАН ЈОКИЋ[1] и НЕБОЈША Д. НИКОЛИЋ[2]

[1]*Технолошко–металуршки факултет, Универзитет у Београду, Карнегијева 4, Београд и* [2]*ИХТМ – Центар за електрохемију, Универзитет у Београду, Његошева 12, Београд*

Поларизационе криве добијене дигиталном симулацијом су корелисане са типом контроле процеса електрохемијског таложења метала у функцији односа густине струје измене и граничне дифузионе густине струје (j_0/j_L). На основу j_0/j_L односа утврђени су дијагностички критеријуми. За $j_0/j_L > 100$, систем је под омском контролом. У опсегу $1 < j_0/j_L \leq 100$ постоји мешовита омско–дифузиона контрола. Дифузиона контрола се јавља у опсегу $0{,}1 < j_0/j_L \leq 1$. За $j_0/j_L \leq 0{,}1$, систем је активационо контролисан на малим пренапетостима. Предложени дијагностички критеријуми су потврђени поређењем симулираних кривих са експериментално снимљеним кривама и анализом морфологија талога добијених у различитим типовима контроле процеса електрохемијског таложења метала.

(Примљено 17. јула, ревидирано и прихваћено 17. септембра 2015)

REFERENCES

1. K. I. Popov, S. S. Djokić, B. N. Grgur, *Fundamental aspects of electrometallurgy*, Kluwer Academic/Plenum Publishers, New York, 2002, p.p. 1–305
2. R. Winand, *Electrochim. Acta* **39** (1994) 1091
3. V. M. Kozlov, L. Peraldo Bicelli, *J. Cryst. Growth* **203** (1999) 255
4. K. I. Popov, M. G. Pavlović, Lj. J. Pavlović, M. I. Čekerevac, G. Ž. Remović, *Surf. Coat. Technol.* **34** (1988) 355
5. A. Damjanović, *Plating* **52** (1965) 1017
6. K. I. Popov, B. N. Grgur, M. G. Pavlović, V. Radmilović, *J. Serb. Chem. Soc.* **58** (1993) 1055
7. K. I. Popov, V. Radmilović, B. N. Grgur, M. G. Pavlović, *J. Serb. Chem. Soc.* **59** (1994) 47
8. K. I. Popov, M. D. Maksimović, J. D. Trnjančev, M. G. Pavlović, *J. Appl. Electrochem.* **11** (1981) 239

9. N. D. Nikolić, K. I. Popov, in *Electrodeposition: Theory and Practice, Series: Modern Aspects of Electrochemistry*, S. S. Djokić, Ed., Vol. 48, Springer, New York, 2010, p. 1
10. K. I. Popov, N. V. Krstajić, *J. Appl. Electrochem.* **13** (1983) 775
11. K. I. Popov, P. M. Živković, N. D. Nikolić, in *Electrodeposition: Theory and Practice, Series: Modern Aspects of Electrochemistry*, S. S. Djokić, Ed., Vol. 48, Springer, New York, 2010, p. 163
12. N. D. Nikolić, K. I. Popov, P. M. Živković, G. Branković, *J. Electroanal. Chem.* **691** (2013) 66
13. N. D. Nikolić, V. M. Maksimović, G. Branković, P. M. Živković, M. G. Pavlović, *J. Serb. Chem. Soc.* **78** (2013) 1387
14. N. D. Nikolić, K. I. Popov, E. R. Ivanović, G. Branković, *J. Serb. Chem. Soc.* **79** (2014) 993
15. J. S. Newman, *Electrochemical Systems*, Prentice-Hall, Inc. Engelwood Cliffs, NJ, 1973, p. 177
16. K. I. Popov, P. M. Živković, B. N. Grgur, *Electrochim. Acta* **52** (2007) 4696
17. J. O' M. Bockris, A. K. N. Reddy, M. Gamboa-Aldeco, *Modern Electrochemistry 2 A*, 2nd ed., Kluwer/Plenum, New York, 2000, p. 1107
18. G. Wranglen, *Electrochim. Acta* **2** (1960) 130
19. H. M. Liaw, J. W. Faust Jr, *J. Cryst. Growth* **18** (1973) 250
20. C. Ding, C. Tian, R. Krupke, J. Fang, *CrystEngComm* **14** (2012) 875
21. R. Sivasubramanian, M. V. Sangaranarayanan, *CrystEngComm* **15** (2013) 2052
22. S. S. Djokić, N. D. Nikolić, P. M. Živković, K. I. Popov, N. S. Djokić, *ECS Trans.* **33** (2011) 7
23. N. D. Nikolić, P. M. Živković, B. Jokić, M. G. Pavlović, J. S. Stevanović, *Maced. J. Chem. Chem. Eng.* **33** (2014) 169
24. J. Han, J. Liu, *J. Nanoeng. Nanomanuf.* **2** (2012) 171
25. M. V. Mandke, S.-H. Han, H. M. Pathan, *CrystEngComm* **14** (2012) 86
26. Z-Y. Lv, A.-Q. Li, Y. Fei, Z. Li, J.-R. Chen, A.-J. Wang, J.-J. Feng, *Electrochim. Acta* **109** (2013) 136
27. V. D. Jović, B. M. Jović, M. G. Pavlović, *Electrochim. Acta* **51** (2006) 5468
28. L. Vazquez-Gymez, E. Verlato, S. Cattarin, N. Comisso, P. Guerriero, M. Musiani, *Electrochim. Acta* **56** (2011) 2237
29. J. Wang, L. Wei, L. Zhang, Y. Zhang, C. Jiang, *CrystEngComm* **14** (2012) 1629
30. V. M. Maksimović, N. D. Nikolić, V. B. Kusigerski, J. L. Blanuša, *J. Serb. Chem. Soc.* **80** (2015) 197.